Power capacity from earcanal dynamic motion

Johan Carioli, Aidin Delnavaz, Ricardo J. Zednik, and Jérémie Voix[a]
Mechanical Engineering Department, École de technologie supérieure,
H3C 1K3 Montreal, Québec, Canada

In-ear devices, such as a hearing aids, electronic earplugs, and wearables, need electrical power to operate. Batteries are the current solution, but unfortunately they also create other problems. For example, several hundred million users, mostly elderly, must change their hearing aid batteries on a weekly basis, which represents not only significant financial costs but a negative environmental impact. A promising alternative involves harvesting energy by converting the dynamic jaw movements into electrical energy via the earcanal. The extent that jaw movements distort the earcanal is still unknown, making it difficult to design the appropriate energy harvesting system for the earplug. Moreover, the finite element methods are barely capable to model the behavior of the earcanal distortion because of the complexity of mechanisms that deform the earcanal. However, this paper presents an alternative method, based on analytical considerations, to understand in-ear mechanical quasi-static deformations using earcanal point clouds. This model quantifies the bending and compressive movements of the earcanal. It can therefore be used to select an appropriate deformation mode for harvesting energy from the earcanal's dynamic motion. The value of this approach was illustrated by calculating the obtainable mechanical energy from 12 human subjects. On average, the bending energy in a human earcanal was found to be three times greater than the radial compression energy. This key finding will need to be considered in the design of future in-ear energy harvesting devices. Such an energy harvesting device has the potential to revolutionize the market for in-ear wearable devices and hearing aids by complementing or replacing battery technology. *© 2016 Author(s). All article content, except where otherwise noted, is licensed under a Creative Commons Attribution (CC BY) license (http://creativecommons.org/licenses/by/4.0/).* [http://dx.doi.org/10.1063/1.4971215]

I. INTRODUCTION

Hearing aids are electronic devices and thus need a power supply to ensure their operation. One of the factors that deteriorate the user's experience is the use of batteries and this is a major challenge for the design of in-ear devices. In addition to the inconvenience and cost, batteries represent a detrimental environmental impact. Various rechargeable battery technologies exist, but the low efficiency and power capacity of rechargeable batteries require that hearing aids be larger or recharged more frequently. Ideally, hearing aids should be self-powered, that is, able to harvest the energy they require from their environment. For in-ear devices, including hearing aids, electronic earplugs, and other wearables, jaw-joint movement appears to be a promising source of mechanical energy.

A. Energy harvesting from human beings

The quantity of harvestable energy contained in the human body is significant.[1,2] Energy can be harvested from body heat, breath, blood pressure, upper limb motion, walking, or finger motion.[3,4] Indeed the energy stored in the human body is available throughout the life of the subject. The head region is of particular interest, due to its proximity to the ear. In this case, the kinetic energy

---

[a]Corresponding author: jeremie.voix@etsmtl.ca.

developed by the earcanal being distorted during a closing jaw movement[5] can be directly harvested by the in-ear device. The conversion of this mechanical energy into electrical energy can be performed using piezoelectric elements. Nevertheless, a more complete understanding of the earcanal's dynamic motion is necessary, in order to efficiently design an in-ear energy harvester suitable to earcanal distortion.

B. Dynamic earcanal movement

The earcanal is unique in each human being and its shape is distorted by dynamic jaw movements.[6] It has been shown that the earcanal changes volume during jaw movement.[7] However, previous investigations fail to understand the strain state in the earcanal. Although finite element simulation has been tried, it is based on geometrical matching between the virtually deformed earpiece model and digitally scanned ear impression model which may not be sufficiently precise.[8] Therefore, the load on earplugs caused by earcanal deformation is still unknown. As it is not yet possible to instrument earplugs with strain-gages, this paper characterizes the earcanal quasi-static deformation by means of ear molds made in the open-mouth and closed-mouth positions.[9,10] These two ear molds were converted to digital point clouds and the relative displacement between the two corresponding positions were computed throughout the point cloud. This analysis assumes that the contact between the earcanal and the custom earplug was coherent. Understanding the strain state in the earplug caused by the jaw motion is an important result. The present investigation therefore focuses on the analysis of this strain state extracted from point clouds taken for the two extreme shapes of the earcanal, that is, at which it reaches a maximum, open-mouth and closed.

C. Strain state from a point cloud

Determining the strain state in deformable solids from shape variations is a major issue in continuum mechanics.[11,12] As the earplug remains in the earcanal during distortion, it is impossible to use Moiré techniques, photoelelasticity, or holographic interferometry. Moreover, although computing the strain state from a scatterplot could be an option,[13,14] this technique is unreliable when the geometry and the load are complex and when it is not possible to understand the stress field in the entire solid. Instead, this study proposes a linear elastic continuum mechanics model to describe the deformation of the earcanal. In this model, a beam theory is used to link the measurable surface displacements to the deformation of the earcanal.[15] For cylinders, the axial load can be linked to the external shape.[16] This analysis helps to understand the bending and radial compression modes exhibited by the earcanal. These two modes of deformation are suitable for existing piezoelectric elements, which can be used to harvest the kinetic energy of the earcanal. This approach does not provide a measure of the torsional deformation, but this is of little consequence since piezoelectric elements are generally not very effective at exploiting torsional strain. The two exploitable modes of deformation are therefore used to calculate the harvestable bending energy and radial compression energy available from earcanal motion.

D. Objectives

This paper aims to explain the behavior of a custom earplug subjected to earcanal distortion due to jaw-joint movement. This entails understanding the strain state in the ear-mold to identify which deformation mode is the most promising for energy harvesting. The specific objectives are:

- Identifying the geometrical parameters involved in the strain state of an earplug subjected to earcanal distortion.
- Computing the bending energy and the radial compression energy from ear-mold point clouds.
- Identifying the deformation mode corresponding to the maximum strain energy available to the earplug.

II. GEOMETRICAL PARAMETERS RELEVANT TO EARCANAL DEFORMATION

The focus being to understanding the strain state within a custom ear mold while it is being subjected to earcanal distortion, it is assumed that the earplug remains static and conforms to the earcanal
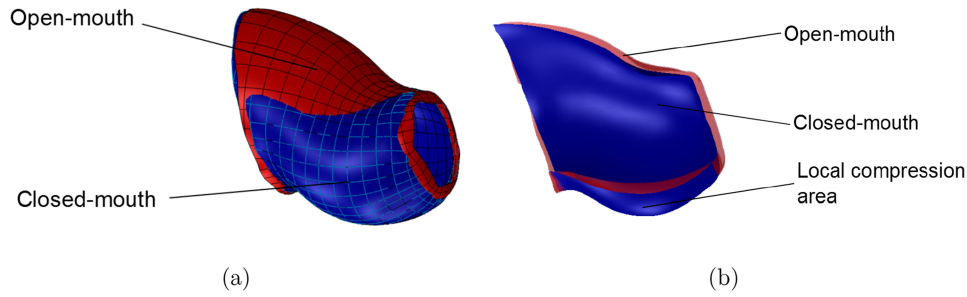
FIG. 1. (a) Earcanal in two extreme positions showing a global bending movement of the earcanal (b) Earcanal sectional view in two extreme positions showing a local compression area of the earcanal.

during the jaw-joint movements. Thus, the behavior of the earplug can be studied by understanding the earcanal's distortion. The earcanal motion caused by jaw-joint movement can be illustrated by superimposing point clouds for two extreme positions: open-mouth and closed-mouth. The earplug has a global bending movement, as shown in Fig. 1(a), and some areas of the custom ear mold are compressed, as shown in Fig. 1(b). The bending movement and the radial compression of the earcanal are quantified by computing the radial compression energy $E_{compression}$ and the bending energy $E_{bending}$ in the custom ear mold for closing cycles. To estimate the in-ear deformation, in terms of bending and radial energy, the two extreme shapes of the earplug are analyzed. The shape of the earplugs in the two extreme positions is compared, as displacements are linked to strain energy. The estimation of the bending energy and the radial compression energy is based on two significant parameters: the curvature of the centroidal axis of the earcanal and the average diameter of the cross-section of the earcanal. The change in curvature between open-mouth and closed-mouth positions is linked to the bending energy of the earcanal. Variations of the average diameter can be related to the radial compression energy. The next section explains how average diameters and curvatures of the earcanal are extracted from ear molds, and how these two parameters are linked to the bending and radial compression energy.

A. Computation of the center axis of the ear mold

The first step consists in extracting relevant parameters from the point clouds of the earcanal. While advanced analysis of complex 3D point clouds is possible,[17] the analysis of the shape of the earcanal from a point cloud was made according to the methodology developed by Stinson et al.[18] It is possible to extract the centroidal axis from the shape of the earplug using an iterative process and then slice the earplug into several cross-sections. In this way, it is possible to compute average diameters, as well as the curvature of the earcanal. The center axis is a space curve designated by $\vec{\gamma}$ and can be described by parametric equations using a sum of trigonometric functions. This space curve is specified in terms of the Cartesian coordinate z as,

$$\vec{\gamma} \equiv \gamma_x \vec{x} + \gamma_y \vec{y} + z\vec{z} \tag{1}$$

where the corresponding x and y components are computed by using the following expressions:

$$\gamma_x(z) = a_1 + a_2 z + a_3 \cos(\beta z) + a_4 \cos(2\beta z) + a_5 \sin(\beta z) + a_6 \sin(2\beta z)$$
$$\gamma_y(z) = b_1 + b_2 z + a_3 \cos(\beta z) + b_4 \cos(2\beta z) + b_5 \sin(\beta z) + b_6 \sin(2\beta z) \tag{2}$$

where $\beta = \frac{\pi}{\Delta z}$, with Δz being the range of z values taken by the data points.

B. Curvature of the center axis

Knowing the shape of $\vec{\gamma}$ makes it possible to study its geometrical characteristics. To do this, the Serret-Frenet frame is defined for each point of the center axis curve by three orthonormal vectors $(\vec{s}, \vec{n}, \vec{b})$. Here $\vec{s}$ is tangent to the center axis, $\vec{n}$ is perpendicular to the center axis and points to the apparent origin of curvature, and $\vec{b}$ is perpendicular to both previous vectors (Fig. 2). The Serret-Frenet formulae are used to analyze the shape of the center axis $\vec{\gamma}$.
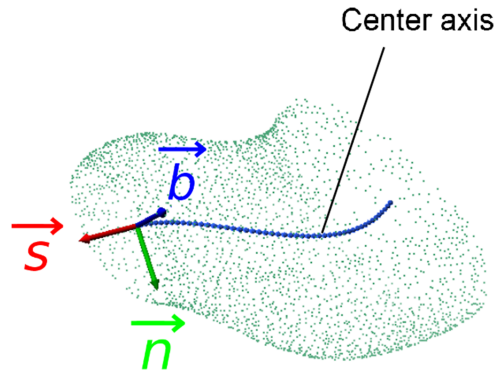
FIG. 2. Earcanal, center axis and Serret-Frenet frame.

The tangent vector $\vec{s}$ is computed using:

$$\vec{s} \equiv \frac{d\vec{\gamma}}{ds} \tag{3}$$

The variation in the tangent vector along the center axis results in the curvature κ in the direction $\vec{n}$

$$\frac{d\vec{s}}{ds} = k\vec{n} \tag{4}$$

By combining Equations (3) and (4), κ can be computed along the center axis by

$$\kappa = \left| \frac{d^2\vec{\gamma}}{ds^2} \right| \tag{5}$$

C. Average diameter of cross-sections of the ear canal

The center axis $\vec{\gamma}$ is used to define the cross-sections of the earcanal. Indeed, point clouds of the earcanal are cut along planes perpendicular to the tangent vector $\vec{s}$. These cross-sections of the earcanal, as illustrated in Fig. 3, are defined as the intersection of these planes and the earcanal point clouds. Given the resolution of the point cloud, the thickness of the cross-sections must be chosen judiciously. Since the external shape of the earcanal is complex, the cross-sections are expected to form elliptical cylinders. Then, for each cross-section, a circular regression is computed. In this way, each cross-section is linked to an average diameter d.
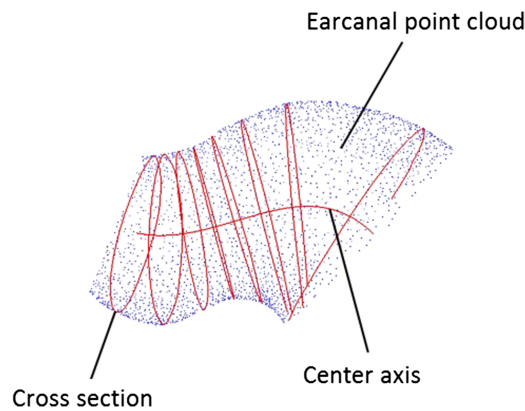

FIG. 3. Earcanal point cloud and associated cross-sections (the three dimensional point cloud is necessarily projected in a two-dimensional plane for illustrative purposes).
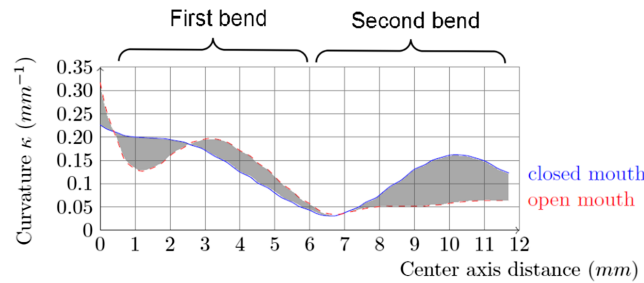
FIG. 4. Curvature alignment of the center axes for the two extreme positions. The area between two curves (in gray) is proportional to the available bending energy.
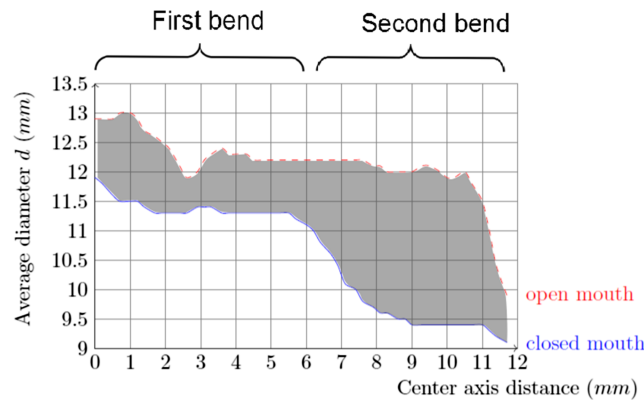

FIG. 5. Diameter alignment of the center axes for the two extremes positions. The area between two curves (in gray) is proportional to the available compressive energy.

D. Comparison of geometrical parameters for the two extreme positions

According to Stinson's previous work,[18] the physiognomy of the human earcanal has two major bends. He found that the location and curvature of these bends do not change among human subjects. These two bends can therefore be identified by finding the local minima of the curvature. It is assumed that during jaw movement, the location of the first bend and the second bend do not change. By using this assumption, the two center axes can be aligned and thereby, comparisons can be made for the center axis curvatures, as shown in Fig. 4, as well as the average diameters, as shown in Fig. 5.

III. METHOD

This section presents an analytical framework to compute the strain energy of a custom earplug from an ear mold point cloud. Both the bending energy and the radial compression energy can be determined from the earplug.

A. Bending energy

Knowing the earcanal's curvature variation makes it possible to compute the bending energy in the earplug induced by the closing jaw-joint movement. The shape of the earplug is assumed to be coherent with the shape of the earcanal. The reference configuration is always the earplug in an open-jaw position and the deformed configuration is the earplug in a closed-jaw position. The initial three dimensional problem is thereby reduced to a two-dimensional axi-symmetrical problem. In this way, it is possible to estimate the bending energy. The earplug is considered as a variable cross-section beam. Curved beam theory[19] is used to link the curvature at the open-mouth position, κ_{open}, and the closed-mouth position, κ_{closed}, to the bending moment. The computation of the bending moment, M,

along the center-axis of the earcanal, is obtained from the following equation:

$$M = EI(s)(\kappa_{\text{open}}(s) - \kappa_{\text{closed}}(s)).$$
(6)

where s corresponds to the distance along the center axis, and where E, the Young's modulus of elasticity, is assumed to be known. The earplug is isotropic and homogeneous. The quadratic moment of cross-section $I(s)$ is computed from the average diameters d_{open} of the cross-sections, measured at the reference position, by the equation:

$$I(s) = \frac{\pi d_{\text{open}}^4(s)}{64}$$
(7)

The bending energy stored in the custom earplug due to a closing-jaw movement is computed using the beam theory:[20,21]

$$E_{\text{bending}} = \frac{E\pi}{128} \int_0^L d_{open}^4(s) \left(\kappa_{\text{open}}(s) - \kappa_{\text{closed}}(s) \right)^2 ds$$
(8)

where L denotes the length of the earcanal.

This equation is discretized to be used in a computational procedure suitable to points clouds:

$$E_{\text{bending}} = \frac{LE\pi}{128N} \sum_{i=1}^{N} d_{open}^4(i) \left(\kappa_{\text{open}}(i) - \kappa_{\text{closed}}(i) \right)^2$$
(9)

where N is the number of cross-sections used to describe the shape of the earcanal.

B. Radial compression energy

The cross-sections of the earcanal vary in shape, depending on whether they correspond to the open-mouth or closed-mouth positions, as shown in Fig. 6. Such variations represent a radial compression of the earcanal and thus, the computation of the radial compression energy from point clouds of open-mouth and closed-mouth positions is possible. The radial compression energy is computed based on the radial stress σ_{rr} in the earplug.

Linear elastic continuum mechanics considerations are used to link the average cross-section diameters to σ_{rr}, and assuming that the earplug is continuous, homogeneous, isotropic, and follows Hooke's Law, the displacements and strains are assumed to be small. The strain state in each section of the earplug is unknown and follows Lamé's equation of elasticity. The stress tensor $\boldsymbol{\sigma}$ is defined as:

$$\boldsymbol{\sigma} = \lambda \text{trace}(\boldsymbol{\varepsilon})I + 2\mu\boldsymbol{\varepsilon}$$
(10)

where, $\boldsymbol{\varepsilon}$ is the strain tensor and λ and μ are the two Lamé coefficients.
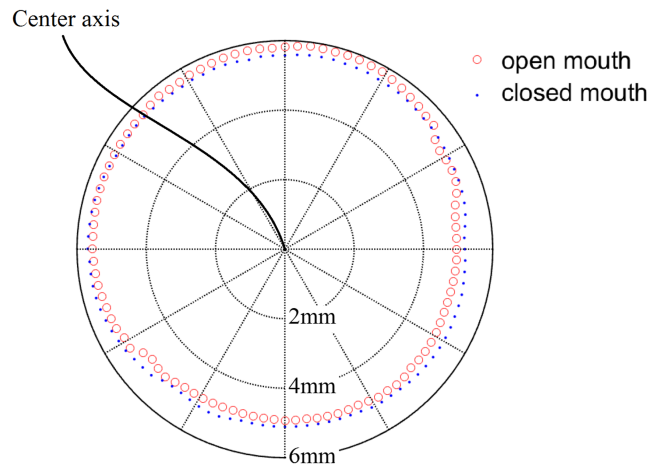

FIG. 6. Comparison of cross-sections of the earcanal for the open-mouth and closed-mouth positions showing the radial compression effect induced by the jaw-joint movement.

These coefficients are related to the mechanical caracteristics the Young's modulus E and the Poisson's ratio ν of the material by:

$$\lambda = \frac{\nu E}{(1 + \nu)(1 - 2\nu)}$$
$$\mu = \frac{\lambda}{2(1 + \nu)} \tag{11}$$

The studied custom earplugs are made of silicon, a type of polymer known to have a Poisson's ratio ν close to 0.5, like most silicon materials that are considered incompressible. This provides:

$$\text{trace}(\boldsymbol{\varepsilon}) = 0 \tag{12}$$

which implies:

$$\boldsymbol{\sigma} = 2\mu\boldsymbol{\varepsilon} \tag{13}$$

Therefore, the initial problem is reduced to an axisymmetric problem. Each slice is modeled by a disk with an external diameter of d_{open}. The action of the earcanal compresses the disc until it has a diameter of d_{closed}. In such a case of axisymmetric plane stress, the equation that governs the field displacement in each slice can be written as:

$$\frac{d^2 u}{dr^2} + \frac{1}{r}\frac{u}{r} - \frac{1}{r^2} = 0 \tag{14}$$

Note that, cylindrical coordinates are used, as they are adapted to the problem's rotational symmetry. The displacement field $u(r)$ is deduced by resolving Equation (14). This field depends on two constants A and B, which depend on the boundary conditions.

$$u(r) = Ar + \frac{B}{r^2} \tag{15}$$

Moreover, the strain tensor $\overline{\overline{\varepsilon}}$ is linked to the field displacement $u(r)$ and can be written as:

$$\boldsymbol{\varepsilon} = \begin{bmatrix} \frac{\partial u(r)}{\partial r} & 0 & \varepsilon_{rz} \\ 0 & \frac{u(r)}{r} & 0 \\ \varepsilon_{rz} & 0 & \varepsilon_{zz} \end{bmatrix} \tag{16}$$

The external displacements of the disk are known and used to determine constants A and B. The displacement field, $u(r)$, is then expressed by:

$$u(r) = \left(\frac{d_{\text{open}}(s) - d_{\text{closed}}(s)}{d_{\text{open}}(s)} \right) r \tag{17}$$

By knowing $u(r)$ and combining Equations (13) and (16), radial strain ε_{rr} and the radial stress σ_{rr} can be evaluated by:

$$\varepsilon_{rr} = \frac{\partial u(r)}{\partial r} = \left(\frac{d_{\text{open}}(s) - d_{\text{closed}}(s)}{d_{\text{open}}(s)} \right) \tag{18}$$

$$\sigma_{rr} = 2\mu\varepsilon_{rr} = 2\mu \left(\frac{d_{\text{open}}(s) - d_{\text{closed}}(s)}{d_{\text{open}}(s)} \right) \tag{19}$$

depending on average diameters of the cross section in the open-mouth position (d_{open}) and in the closed-mouth position (d_{closed}). Therefore, the radial strain energy $dE_{\text{compression}}$ energy in one cross-section can be computed by

$$dE_{\text{compression}} = \frac{1}{2}\varepsilon_{rr}(s)\sigma_{rr}(s)\frac{\pi d_{\text{closed}}^2(s)}{4}ds \tag{20}$$

Then, the compression energy $E_{\text{compression}}$ stored in the earplug is computed as follows and depends on L, the length of the earcanal.

$$E_{\text{compression}} = \int_0^L \frac{\mu\pi(d_{\text{open}}(s) - d_{\text{closed}}(s))^2}{4} ds \tag{21}$$

This equation is discretized to be used in a computational procedure suitable to points clouds:

$$E_{\text{compression}} = \frac{L}{N} \sum_{i=1}^{N} \frac{\mu \pi (d_{\text{open}}(i) - d_{\text{closed}}(i))^2}{4} \tag{22}$$

where, N is the number of cross-sections used to describe the shape of the earcanal.

IV. IMPLEMENTING THE FRAMEWORK FOR EAR CANAL DEFORMATION

The present work develops a computational procedure to estimate the earcanal deformation from point clouds in two extreme positions. Equations (9) and (22) are used to process the point clouds from the custom ear molds made using the Sonofit proprietary process[22] for both ears of 12 human subjects. Ear molds were digitized using a 3D laser coordinate measuring machine (CMM). The computational procedure for the analysis of earcanal deformation can support various parameters, depending on the mechanical problem being studied. Indeed, the silicon can be adapted to improve the strain energy stored in the earplug. Here, the mechanical characteristics of the silicon, type MED-4910 (NuSil Technology, USA) are known. Moreover, the accuracy of the results depends on the number of cross-sections. In this paper, the parameters used are described in Table I.

This presented computational procedure for the ear canal deformation analysis can support various parameters depending on the studied mechanical problem. Indeed, the silicon can be adapted to improve the strain energy stored in the earplug. Here the mechanical characteristics of the silicon, type MED-4910 (NuSil Technology, USA) are known. Moreover, the results accuracy depends on the number of cross-sections. In this paper, the paremeters used are described in Table I.

In the interest of brevity, only the compression energy and bending energy are displayed in Table II; obviously, all the intermediate equations are evaluated during the model computation. It is therefore possible to have access to the radial stress σ_{rr}, the radial strain ε_{rr}, and the bending moment M, if needed.

These results show that the bending energy is on average three times greater than the radial compression energy, although this does depend on the subject being studied. Indeed, the standard deviation is about 4.9 mJ while the average energy is about 5 mJ. Moreover, in some cases, the radial compression energy is three times greater than the bending energy. Note that for subject 06, the proportion between bending energy and radial compression energy can be inverted in the same subject for right ear and left ear, confirming that this subject has asymmetric ears.

V. RESULTS AND DISCUSSIONS

Mechanical modeling of an earplug subjected to the earcanal distortion produced the Equations (9) and (22). These equations are used to understand the behavior of a custom earplug that is within the earcanal during jaw movement. Moreover, this analytical method links the curvature variations to the center axis of the earcanal and the bending moment M of the custom earplug. The bending energy and the radial compression energy were quantified as the two principal modes of deformation of the earplug. These equations are designed to process point clouds from custom ear molds in open-mouth and closed-mouth positions. An illustrative implementation of this framework was used to study an ear deformation database containing 12 human subjects. In general, we found that the bending energy is on average three times greater than the radial compression energy, although

TABLE I. Model parameters.

Parameter	Symbol	Value
Silicon's Young's modulus	E	0.89 MPa
Silicon's Lamé coefficient	μ	0.29 MPa
Cross-sections thickness		0.2 mm
Cross-sections number		50

TABLE II. Bending energy, radial compression energy and their proportions for the left (L) and right (R) ears of 12 subjects (3 Females, 9 Males, age between 24 and 60).

Test subject	Bending energy		Radial compression energy	
Ear	Absolute (mJ)	Proportion (%)	Absolute (mJ)	Proportion (%)
01R	3.4	100	0	0
01L	4.7	100	0	0
02R	3.0	96.8	0.1	3.2
02L	1.1	61.1	0.7	38.9
03R	15.1	87.3	2.2	12.7
03L	4.4	93.6	0.3	6.4
04R	4.7	79.7	1.2	20.3
04L	2.5	55.6	2.0	44.4
05R	9.2	100	0	0
05L	19.6	94.2	1.2	5.8
06R	6.8	68.7	3.1	31.3
06L	1.9	41.3	2.7	58.7
07R	1.6	22.9	5.4	77.1
07L	3.1	88.6	0.4	11.4
08R	2.8	50.9	2.7	49.1
08L	1	83.3	0.2	16.7
09R	0.7	100	0	0
09L	7.0	63.1	4.1	36.9
10R	3.0	88.2	0.4	11.8
10L	3.4	59.6	2.3	40.4
11R	2.6	48.1	2.8	51.9
11L	14.6	98.0	0.3	2.0
12R	0.6	85.7	0.1	14.3
12L	3.0	96.8	0.1	3.2
Mean	5	77.6	1.3	22.4
Std. dev	4.9	22.2	1.5	22.2

with considerable variation between subjects. The wide variation of results can be explained in light of the specifics of the earcanal shape, which is unique in every human being. Both the shape of the earcanal and also the morphology of the temporomandibular joint influence the strain state in the earplug. Although the specificity of the distortion of the earcanal to every human was previously known, breaking down this deformation into the bending and radial compression modes is a major step forward. Moreover, in a previous study, volume variations of the earcanal were computed from the point cloud database. This database had never been used to compute stress-strain fields, which is unique to this study. The analytical model developed is based on linear elastic continuum mechanics and the assumption that the contact between the earcanal and the custom earplug are coherent; meaning that all the displacements of the earcanal caused by the jaw-closing movement are transmitted to the custom earplug. The strain energy stored in the earplug due to temporomandibular movements can be interpolated from the earcanal point clouds in the two extreme positions. These results are an estimation of the behavior of an earplug subjected to the earcanal's dynamic motion. As the mechanical load imposed by the temporomandibular movement is still unknown, finite element methods fail to understand the behavior of the earcanal. This framework provides a novel approach to describing the human earcanal that is invaluable for the quantitative characterization of earcanal deformation. In particular, it can be used to identify the appropriate deformation mode for harvesting energy from the earcanal's dynamic motion.

VI. CONCLUSION

An analytical framework to estimate the behavior of custom earplugs in the earcanal has been developed. This calculation computes the bending energy and the radial compression energy from

point clouds of the earcanal in the open-mouth and closed-mouth positions. This method is based on an analytical model of the deformations of the custom earplug. Even if the mechanical load imposed by the temporomandibular movement on the earcanal is still unknown, the model predicts the mechanical behavior of a custom earplug in the earcanal during the closing-jaw movement. Applying this framework to a database of human earcanals shows that the bending energy is generally three times greater than the radial compression energy, and therefore should be used for earcanal energy harvesting. Future work should focus on designing an in-ear energy harvester from this mechanical bending of the earcanal. In addition, measuring the mechanical load imposed by the earcanal, and verifying the contact behavior between the earplug and the earcanal may be useful.

ACKNOWLEDGMENTS

[1] E. Romero, R. O. Warrington, and M. R. Neuman, "Energy scavenging sources for biomedical sensors," Physiological Measurement **30**, R35–R62 (2009).
[2] M. Pozzi and M. Zhu, "Plucked piezoelectric bimorphs for knee-joint energy harvesting: modelling and experimental validation," (2011).
[3] T. Starner, "Human-powered wearable computing," IBM systems Journal **35**, 618–629 (1996).
[4] J. A. Paradiso and T. Starner, "Energy scavenging for mobile and wireless electronics," IEEE Pervasive computing **4**, 18–27 (2005).
[5] V. K. Varadan, *Smart Material Systems and MEMS: Design and Development Methodologies* (John Wiley & Sons, Chichester, Angleterre, Hoboken, NJ, 2006).
[6] D. J. Cunningham, *Cunningham's Textbook of Anatomy* (W. Wood, 1818).
[7] A. Delnavaz and J. Voix, "Energy harvesting for in-ear devices using ear canal dynamic motion," IEEE Transactions on Industrial Electronics **61**, 583–590 (2014).
[8] A. Delnavaz and J. Voix, "Piezo-earpiece for micro-power generation from ear canal dynamic motion," Journal of Micromechanics and Microengineering **23**, 114001 (2013).
[9] M. J. Grenness, J. Osborn, and W. L. Weller, "Mapping ear canal movement using area-based surface matching," The Journal of the Acoustical Society of America **111**, 960–971 (2002).
[10] S. Darkner, R. Larsen, and R. R. Paulsen, "Analysis of deformation of the human ear and canal caused by mandibular movement," *International Conference on Medical Image Computing and Computer-Assisted Intervention* (Springer, 2007), pp. 801–808.
[11] G. S. Holister, *Experimental Stress Analysis : Principles and Methods*, Cambridge Engineering Series (Cambridge University Press, London, 1967).
[12] A. S. Khan, *Strain Measurements and Stress Analysis* (Prentice Hall, Upper Saddle River, NJ, 2001).
[13] F. Heuer, U. Wolfram, H. Schmidt, and H.-J. Wilke, "A method to obtain surface strains of soft tissues using a laser scanning device," Journal of Biomechanics **41**, 2402–2410 (2008).
[14] J. Qian and J. Lu, "Point-cloud method for image-based biomechanical stress analysis," International Journal for Numerical Methods in Biomedical Engineering **27**, 1493–1506 (2011).
[15] R. Glaser, V. Caccese, and M. Shahinpoor, "Shape monitoring of a beam structure from measured strain or curvature," Experimental Mechanics **52**, 591–606 (2011).
[16] Z. Wei-zhou, S. Shun-cheng, C. Gang, H. Xi-cheng, and H. Peng, "Stress field of orthotropic cylinder subjected to axial compression," Applied Mathematics and Mechanics **31**, 305–316 (2010).
[17] H. Huang, S. Wu, D. Cohen-Or, M. Gong, H. Zhang, G. Li, and B. Chen, "L1-medial skeleton of point cloud," ACM Trans. Graph. **32**, 65–1 (2013).
[18] M. R. Stinson and B. W. Lawton, "Specification of the geometry of the human ear canal for the prediction of soundpressure level distribution," The Journal of the Acoustical Society of America **85**, 2492–2503 (1989).
[19] R. Subramanian, *Strength of Materials*, 2nd edition (Oxford University Press, 2010).
[20] S. Timoshenko, *Theory of Elasticity*, 3rd ed., Engineering societies monographs (McGraw-Hill, New York, NY, 1987).
[21] S. Timoshenko, *Elements of Strength of Materials*, 4th ed. (DVan Nostrand, Princeton, NJ, 1962).
[22] I. McIntosh and R. Saulce, "Expandable in-ear device," (2004), u.S. Classification 381/322, 381/325, 381/328; International Classification H04R25/00; Cooperative Classification H04R25/656, H04R25/658; European Classification H04R25/65B, H04R25/65M.